Applications of ocean-bottom seismic recordings

Brian H. Hoffe, Laurence R. Lines and Peter W. Cary

ABSTRACT

Ocean-bottom cable (OBC) recording has led to avenues in elastic wave imaging in marine environments. In this paper, we review many of these applications including:

1. Suppression of receiver-side multiples with dual-sensors.

2. Enhanced imaging using compressional to shear (P-S) converted waves.

3. The attenuation of free-surface multiples using combined streamer and ocean-bottom recordings.

In this review, we describe theory, models, and real data applications for elastic wave imaging of ocean-bottom seismic recordings.

INTRODUCTION

In recent years, there has been much interest in seismic imaging within the marine environment via four-component (4C) OBC recordings. The 4C OBC sensor is equipped with a single hydrophone (pressure detector) plus a three-component (3C) geophone (particle velocity detector). The 3C geophone records the full three-dimensional ground motion via one vertical component and two orthogonal horizontal components. The use of 4C OBC recordings has several advantages over conventional towed streamer technology which include:

1. Dual-sensor summation (hydrophone + vertical geophone signals) for the suppression of receiver-side multiples.

2. Utilising P-S wave conversions for enhanced imaging.

3. Attenuation of free-surface multiples when combined with towed streamer recordings.

We explore many of these elastic wave imaging possibilities from a simple mathematical viewpoint and give synthetic and real data examples for these applications.

MARINE SEISMIC WAVEFIELDS

In examining marine seismic wavefields, we refer the reader to some excellent discussions of the topic by Loewenthal et al. (1985) and Paffenholz and Barr (1995). For the simplest situation, we examine the case shown in Figure 1 of a hydrophone and a geophone located at the ocean-bottom, and assume vertical raypaths through the water column. We use the following notation from Paffenholz and Barr (1995):

P = wavefield pressure.

V = velocity of displacement.

U = upgoing wavefield.

D = downgoing wavefield.

ρ = density of water.

c = acoustic wave velocity of water.

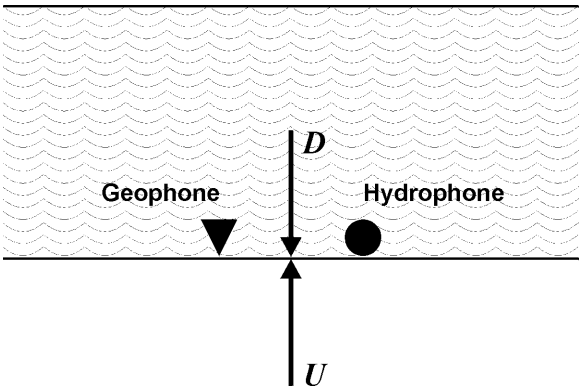

Figure 1. Hydrophone and geophone are located at the ocean-bottom and record the vertically travelling upgoing (***U***) and downgoing (***D***) wavefields.

By using the one-dimensional wave equation, Loewenthal et al. (1985) show that pressure waves are given by:

$$P = U + D \tag{1}$$

and the velocity of displacement wavefield is given by:

$$V = \frac{1}{\rho c}(U - D) \tag{2}$$

Pressure is a scalar quantity, which is independent of the U or D directions. The total wavefield pressure is given by the sum of pressure from the upgoing and downgoing wavefields. A hydrophone is a recording device (usually piezoelectric) which measures wavefield pressure. It is insensitive to the wave's direction and therefore detects no difference between an upgoing compression and a downgoing compression.

Velocity of displacement is a vector quantity and therefore is influenced by wave direction. A geophone measures velocity of a wave's displacement and detects a difference in sign between an upgoing compression and a downgoing compression. The sign convention is somewhat arbitrary and depends on the definition of the co-ordinate system. Like the rule of driving on the left-hand or right-hand side of the road, the sign convention is arbitrary but important to know. For the purposes of this discussion, we will choose a downward travelling compression to be positive and we will multiply V by a scalar constant ρc so as to use $V = U - D$ in subsequent discussions.

USE OF DUAL-SENSORS FOR MULTIPLE SUPPRESSION

The combined use of hydrophones and geophones at the ocean-bottom essentially leads to the use of a "dual-sensor". The combined usage of the hydrophone or pressure recording, P, and the vertical geophone or displacement velocity recording, V, allows us to suppress receiver-side multiples. For the purpose of clarity, Figure 2 illustrates the multiple nomenclature used in this paper. The concept of dual-sensors has been explored by Loewenthal et al. (1985), Barr and Sanders (1989), Dragoset and Barr (1994), and Paffenholz and Barr (1995) among others. These analyses usually assume vertical wave propagation through the water column, but sometimes

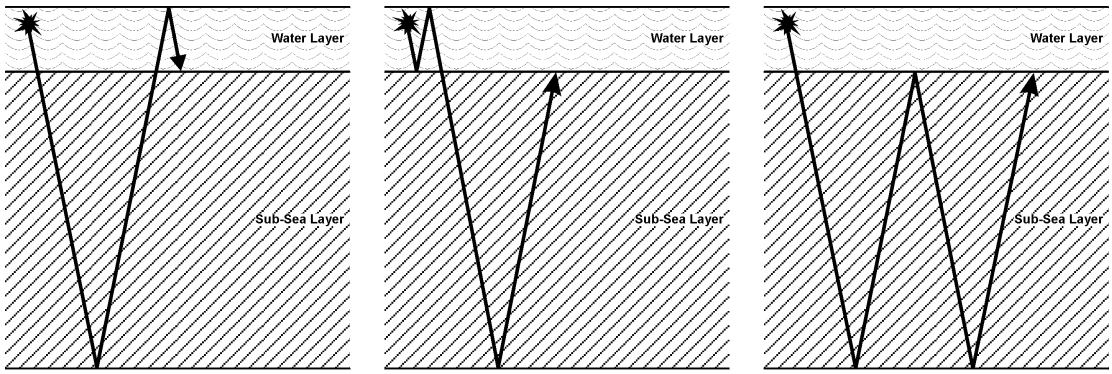

Figure 2. Multiple nomenclature used in this paper: (a) receiver-side multiples, (b) source-side multiples and (c) interbed multiples. Note that the receiver-side multiples would consist of downgoing energy whereas both source-side and interbed multiples would consist of upgoing energy.

allow non-vertical propagation above an acoustic sea floor. A theoretically complete analysis of water-layer multiple attenuation with 4C receivers (hydrophone + 3C geophone) on an elastic sea floor, which includes the dual-sensor situation considered here, has been presented by Osen et al. (1999) among others.

To see how dual-sensors can suppress water-trapped energy consider Figure 3, which depicts a wavefield trapped in a water layer, with a surface reflection coefficient of –1 for reflected pressure waves impinging upon this free surface from below, and a reflection coefficient of R for pressure waves reaching the ocean-bottom from above. We consider the downgoing and upgoing waves at the ocean-bottom for a water layer with two-way traveltime τ and we consider the initial downgoing compressional wavefield to be initiated at time $t = -\tau/2$ so that $t = 0$ occurs when the first arrival impinges on the ocean-bottom with unit amplitude +1. Upon arrival at the ocean-bottom, the wave is partially reflected upward as a compression with amplitude R. It travels upward for time $\tau/2$ before being reflected downward from the ocean surface as a rarefraction with amplitude $-R$ before arriving at the ocean-bottom at time τ, where it is again reflected upward as a rarefraction with amplitude $-R^2$. These water-trapped arrivals continue as a series of reflections with diminishing amplitudes and alternating signs. If we let Z be the delay operator for two-way travel through the water layer, we can consider z transforms for the downgoing and upgoing waves.

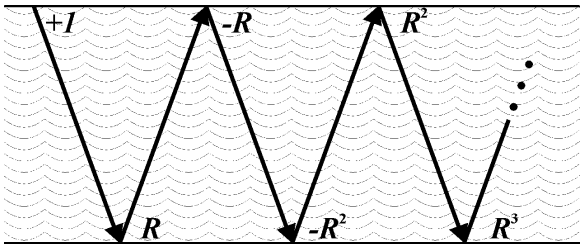

Figure 3. Reverberatory sequence for water-trapped seismic arrivals. Note the alternating sign and diminishing amplitudes ($R < 1$).

At the ocean-bottom, the downgoing wave's z transform is given by:

$$D(Z) = 1 - RZ + R^2Z^2 + \ldots = \frac{1}{1+RZ} \tag{3}$$

and the upgoing wave's z transform is given by:

$$U(Z) = R - R^2Z + R^3Z^3 + \ldots = \frac{R}{1+RZ} \tag{4}$$

The z transform for the pressure wavefield, as recorded by the hydrophone, is given by $P(Z) = U(Z) + D(Z)$ or:

$$P(Z) = \frac{1+R}{1+RZ} \tag{5}$$

The z transform for the velocity of displacement wavefield, as recorded by the geophone, (to within a scalar multiplier ρc) is given by $V(Z) = U(Z) - D(Z)$ or:

$$V(Z) = \frac{R-1}{1+RZ} \tag{6}$$

By inspection of equations (5) and (6), we see that:

$$P(Z) + \frac{(1+R)}{(1-R)}V(Z) = 0 \tag{7}$$

In other words, a summation of the hydrophone recording which measures pressure with a scaled version of the vertical geophone recording which measures velocity of displacement removes one type of multiple. The dual-sensor combination of the hydrophone and vertical geophone recordings will cancel out all receiver-side multiples, while preserving reflections from below the ocean-bottom interface.

This can be illustrated by considering Figure 4 where the upgoing reflectivity's z transform is given by $\beta = \sum R_n z^n$. (Note that we use lower case z in the z transform since the delay operator for the time sampled reflectivity will generally not coincide with the delay operator for the multiples, i.e. $Z = z^\tau$). We can consider the upgoing wavefield, β, to be filtered by the multiples so that the z transform for the upgoing wavefield at the ocean-bottom, as shown in Figure 4, is given by:

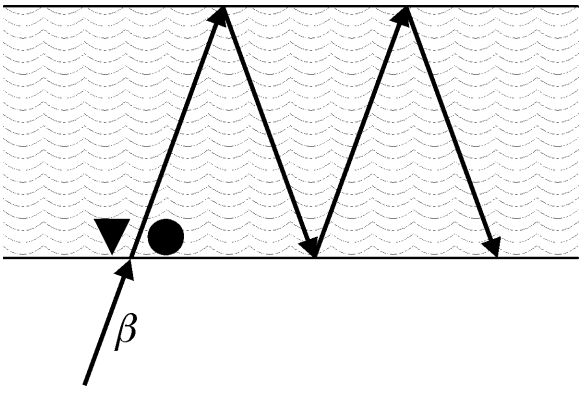

Figure 4. Upgoing reflectivity, β, and subsequent receiver-side multiples.

$$U(Z) = \left(1 - RZ + R^2Z^2 + \ldots\right)\beta = \frac{\beta}{1+RZ} \tag{8}$$

and the downgoing wavefield is:

$$D(Z) = \left(-Z + RZ^2 - R^2Z + \ldots\right)\beta = \frac{-Z\beta}{1+RZ} \tag{9}$$

so that

$$P(Z) = \frac{1-Z}{1+RZ}\beta \tag{10}$$

and

$$V(Z) = \frac{1+Z}{1+RZ}\beta \tag{11}$$

Adding these wavefields as before in equation (7) we obtain:

$$P(Z) + \frac{1+R}{1-R}V(Z) = \frac{2}{1-R}\beta \tag{12}$$

Therefore, the addition of hydrophone and scaled vertical geophone leaves the reflectivity intact (except for a constant factor) while cancelling out the receiver-side multiples. Source-side multiples will still remain in the data. Notice that addition of the hydrophone and geophone without any scaling cancels out the receiver ghost, and leaves both receiver-side and source-side multiples, so the OBC data can be converted to ordinary streamer data in this fashion. With either strategy, the multiples that remain after the dual-sensor data have been combined generally need to be attacked by a more traditional multiple attenuation technique.

1) Synthetic Example

A synthetic example of how receiver-side multiples can be attenuated by the use of dual-sensor technology is illustrated in Figure 5. This figure shows a comparison between the synthetic seismograms computed for the hydrophone, Figure 5(a), scaled vertical geophone, Figure 5(b) and their dual-sensor summed result, Figure 5(c). These seismograms were computed from a general elastic wave model obtained by using P-wave and S-wave sonic logs from the Jeanne d'Arc Basin, offshore Newfoundland. As is evident from Figure 5, both the hydrophone and scaled vertical geophone data show a large number of various water layer multiples between 600 and 1600 ms but are greatly reduced on the dual-sensor summed result. We also note the presence of P-S converted arrivals on all three seismograms of Figure 5. Images of these converted wave arrivals prove useful in marine seismic imaging, as we will see in the next section.

It is important to re-iterate that the dual-sensor method can only directly remove receiver-side multiples (i.e. downgoing multiples) and **not** other types of water-layer multiples as illustrated in Figure 2. Although Equation (12) clearly demonstrates that

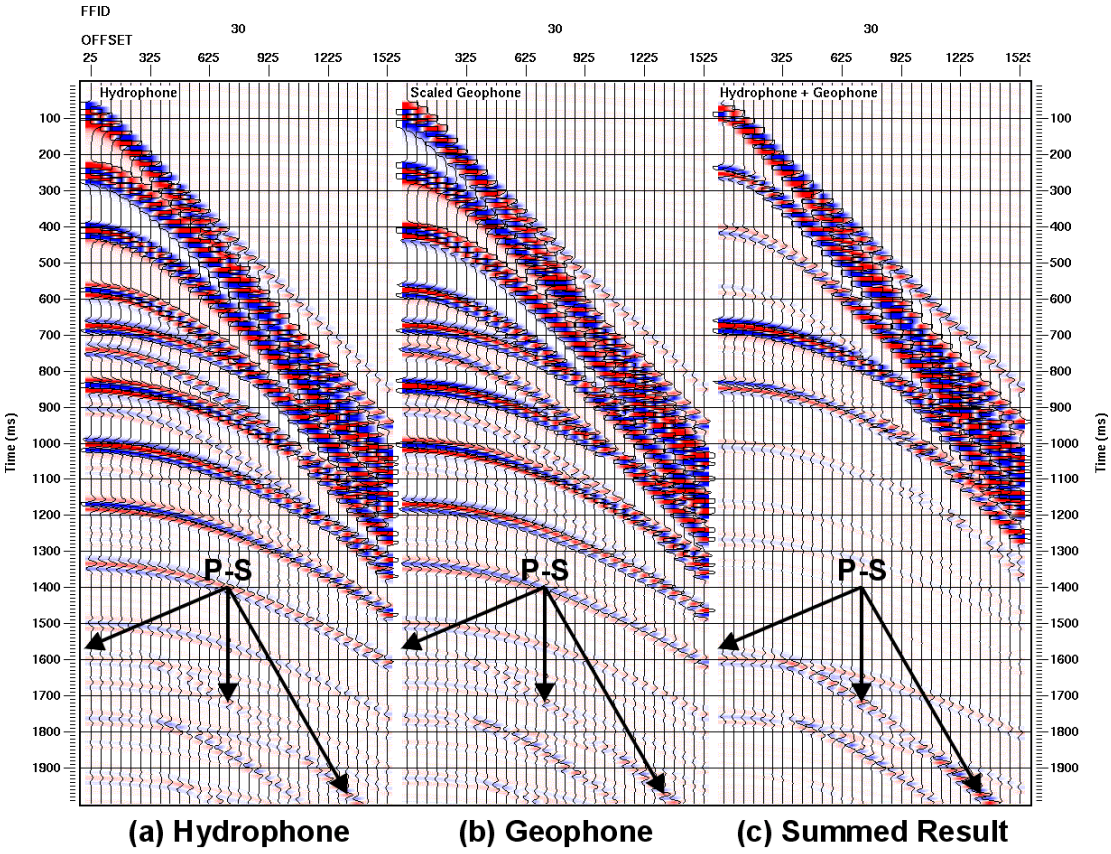

Figure 5. Synthetic OBC seismic data computed from a general elastic wave model of the Jeanne d'Arc Basin for offsets 25-1525 m. (a) hydrophone source gather and (b) the scaled geophone source gather and (c) the dual-sensor summation result. Note on (c) how the receiver-side multiples are greatly reduced in amplitude. Also, both (a), (b) and (c) show the presence of strong, mode-leaked, converted-wave arrivals (labelled "P-S") from the top of the 2nd sub-sea layer.

the summation leaves the upgoing reflectivity intact, this reflectivity is usually contaminated by both source-side and interbed multiples (i.e. upgoing multiples).

This limitation of the dual-sensor method can be examined from a more physical view point as illustrated in Figure 6. This figure displays a zoomed portion of the dual-sensor summed seismogram of Figure 5(c) between 600 and 2200 ms. Although the receiver-side multiples are greatly reduced in amplitude, there are still a number of other water-layer multiples which are not. These other multiple types are identified on the seismogram by their corresponding raypath schematic.

Elaborating further on our sign conventions, we chose the hydrophone to measure a compression as positive and rarefraction as negative. We chose the vertical geophone to measure a downgoing compression as positive, downgoing rarefraction as negative, upgoing compression as negative and upgoing rarefraction as positive. As Figure 6 indicates, since the upgoing reflectivity is contaminated by either source-side multiples, interbed multiples or a combination of both, the hydrophone and vertical geophone will record this upgoing multiple energy with the same sign (i.e. hydrophone compression = geophone upgoing compression = negative; hydrophone rarefaction = geophone upgoing rarefaction = positive). Thus, upon summation of the

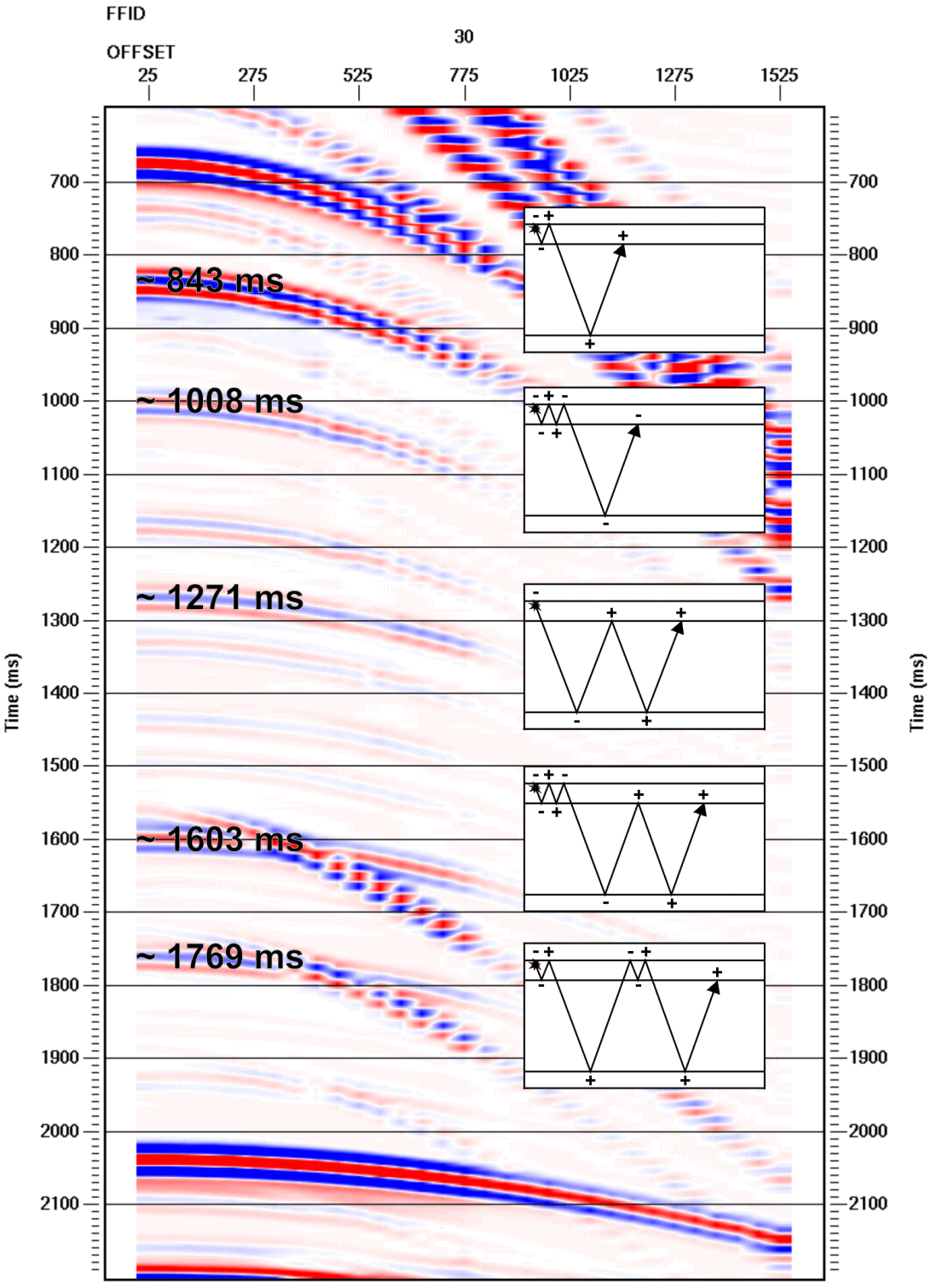

Figure 6. Zoomed portion of Figure 5(c) showing various water-layer multiples and their corresponding raypath schematic which have not been suppressed by dual-sensor summation. These other multiple types are either source-side, interbed or a combination of both (i.e. upgoing multiple energy).

hydrophone and scaled vertical geophone signals, these multiple types will constructively add. This is why there is residual multiple energy after summation.

2) Real Data Example

A real data example of dual-sensor combination is provided by the hydrophone and vertical geophone components of a 4C OBC survey acquired by Geco-Prakla over the Mahogany Field, Gulf of Mexico (Caldwell et al., 1998). Figure 7 shows a portion of a receiver gather from this survey. Prominent primary events are visible on both the hydrophone traces, Figure 7(a), and the geophone traces, Figure 7(b) at near offset arrival times of about 1190 ms and 1690 ms. The water depth is about 120 m, so the ghost, as well as the first receiver-side and source-side multiples, all arrive about 160 ms after each primary event. The second multiple event is also visible about 160 ms later. Notice that the primaries are in phase and the multiples are out of phase on the two components. Also notice that the amplitude of the first multiple on the hydrophone component is actually higher than the amplitude of the primary, which is in accordance with theory when the sea-floor reflection coefficient is positive (about 0.4 in this case). The summed result in Figure 7(c) shows a considerable reduction in the amplitude of the multiples compared to the primaries. However, source-side multiple energy remains, as expected.

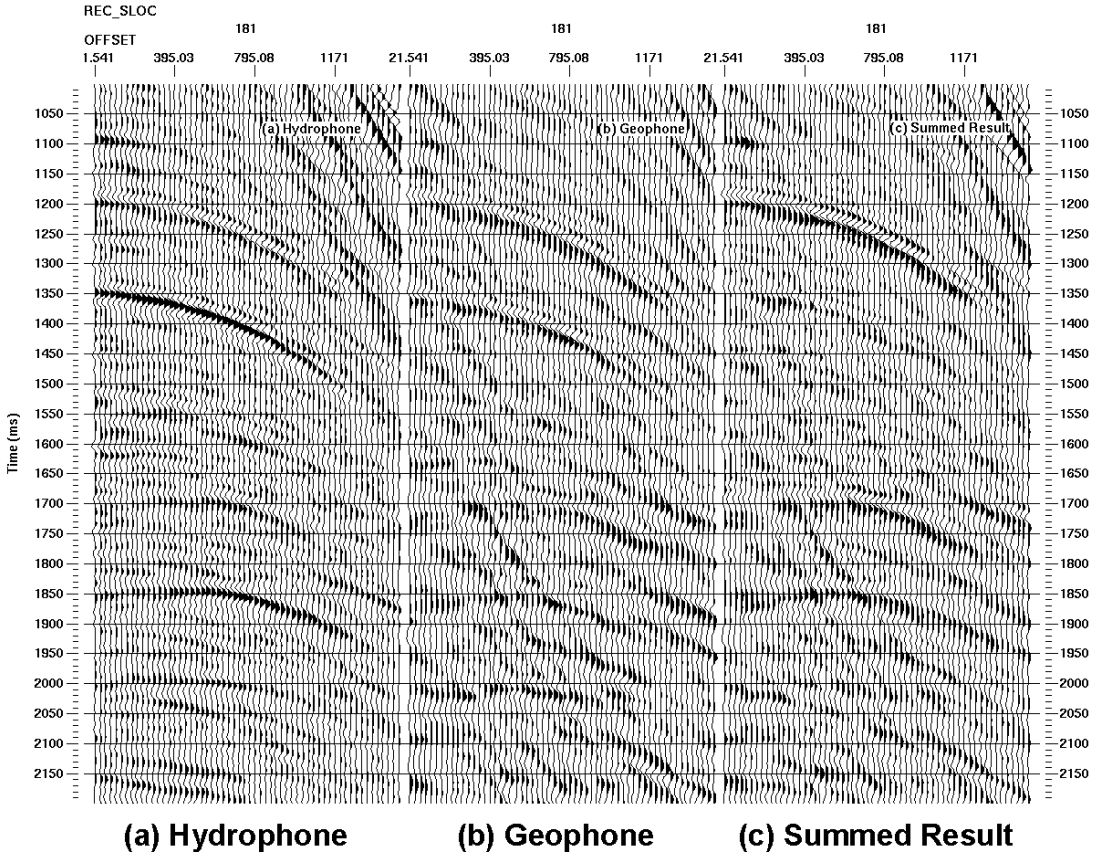

Figure 7. OBC seismic data acquired from the Mahogany field, Gulf of Mexico. (a) hydrophone data, (b) geophone data and (c) summed result. Note the considerable reduction in the amplitude of the multiples compared to the primaries between 1190 ms and 1690 ms.

USING CONVERTED WAVES TO ENHANCE IMAGING

1) Imaging Through Gas-Filled Sediments

Recent case histories from some of the North Sea fields have documented improved seismic imaging through gas-filled sediments using marine converted wave data with startling results. An excellent example of this is provided by Granli et al. (1999).

The Tommeliten chalk fields are located in the southern North Sea and have substantial gas chimneys (~ 2 km wide) associated with them. These chimneys are caused by up-dip leakage of gas along faults which extend from the reservoir level into the overlying sediments. The presence of these gas-charged sediments severely distorts the P-wave seismic image obtained from previous conventional 3D streamer surveys. White (1975) demonstrated that the presence of gas in the subsurface has a strong effect on P-waves. The reason for this, as Granli et al. (1999) points out, is that the bulk modulus, defined as the degree to which a rock is resistant to compression, is a key constituent in the definition of P-wave velocity (i.e. $V_p = \sqrt{\left(k + \frac{4}{3}\mu\right)/\rho}$ where k, μ and ρ are the bulk modulus, shear modulus and density respectively) and is severely distorted in the presence of gas. Small amounts of gas will seriously affect both the traveltime and reflection amplitude for P-waves and, unfortunately, processing of these type of data can only marginally compensate for this effect.

To resolve this imaging problem at the Tommeliten fields, Granli et al. (1999) turned to marine multicomponent OBC recordings in order to better image the reservoir using converted or P-S data. The presence of gas usually has a small effect on the rock density and no significant effect on its shear modulus. The shear modulus is generally defined as the degree to which a rock is resistant to deformation and is the key constituent in the definition of the S-wave velocity (i.e. $V_s = \sqrt{\mu/\rho}$). Thus, S-waves produced via mode-conversion are much less affected by the presence of gas than P-waves.

Figure 8 provides a comparison of the migrated P-S CCP (common conversion point) stack versus the P-P CMP (common midpoint) stack from the Tommeliten field. The CCP stack was produced from the newly acquired OBC converted wave data whereas the CMP stack was produced from previous acquired conventional 3D streamer P-wave data. As Granli et al. (1999) demonstrate and which is clearly evident from Figure 8, converted waves can be used to successfully image through a gas chimney. Also, they point out that the most important mode conversion observed in the marine multicomponent data from the Tommeliten field is conversion from P to S at the reservoir level.

2) Poor P-P Reflectivity

Another excellent case history, also from the North Sea, documenting enhanced seismic imaging using converted waves when there is poor P-P reflectivity is given by MacLeod et al. (1999).

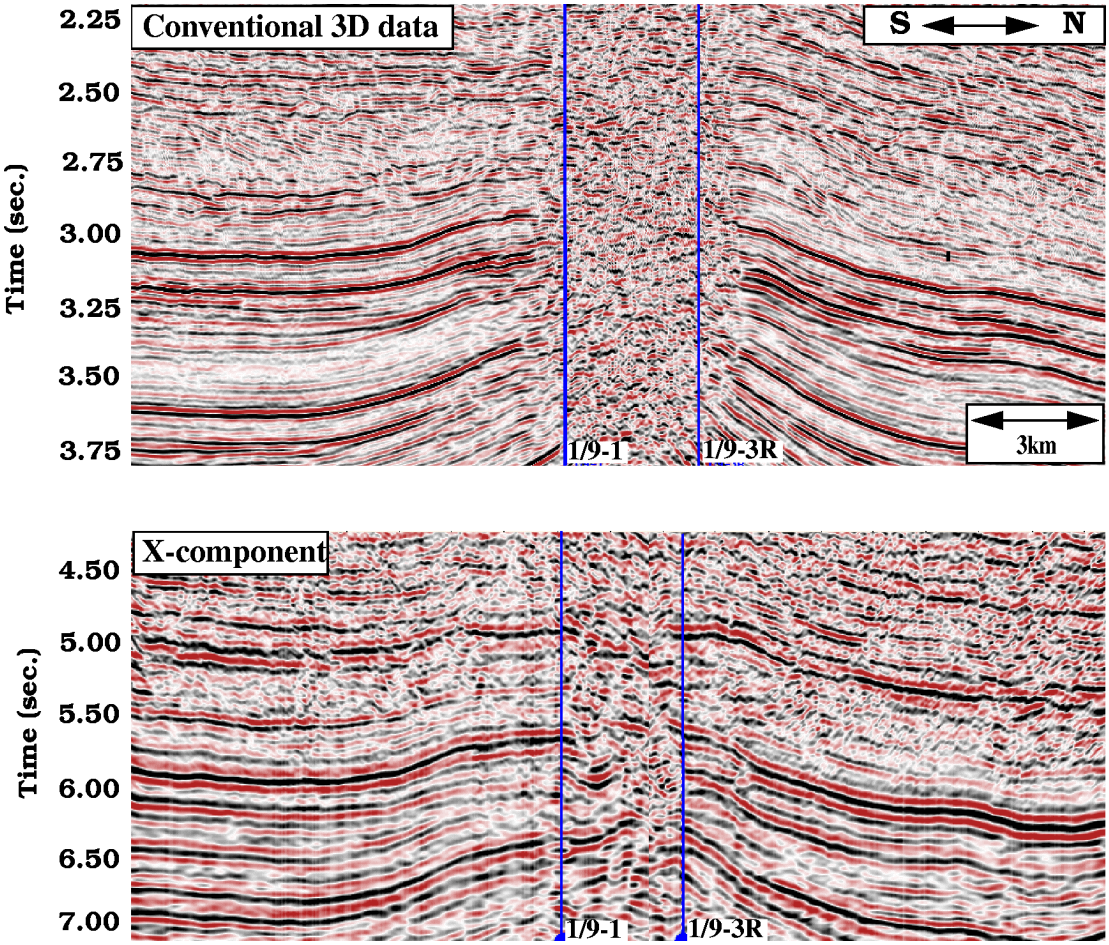

Figure 8. Comparison of P-P CMP (top panel) stack produced from the 3D streamer data and P-S CCP (bottom panel) stack produced from the OBC data for the Tommeliten field. Note how the P-S stack produces a much better image in the presence of gas versus the P-P image (from Granli et al., 1999).

The Alba field is located in the central North Sea. The producing reservoir is a poorly consolidated Eocene turbidite channel sand that can be up to 100 m thick and has an average subsea depth of 2000 m. This channel contains intra-reservoir shales that can cause significant drilling and production problems as the oil production comes from several horizontally-drilled wells.

Since it was critical that the horizontal wells be placed as close to the top of the reservoir as possible, MacLeod et al. (1999) required accurate maps of the reservoir top as well as the location of the intra-reservoir shales. This mapping was extremely difficult using the pre-existing streamer data since the reservoir top is a weak and inconsistent seismic event and the intra-reservoir shales are often seismically invisible.

At Alba the shale-oil interface is extremely difficult to map using conventional P-wave streamer data because the oil sands and shales have, on average, the same acoustic impedance (MacLeod et al., 1999). A dipole sonic log acquired through the reservoir showed a significant S-wave impedance contrast at both the top and bottom of the reservoir. Subsequent seismic modelling using this dipole sonic information

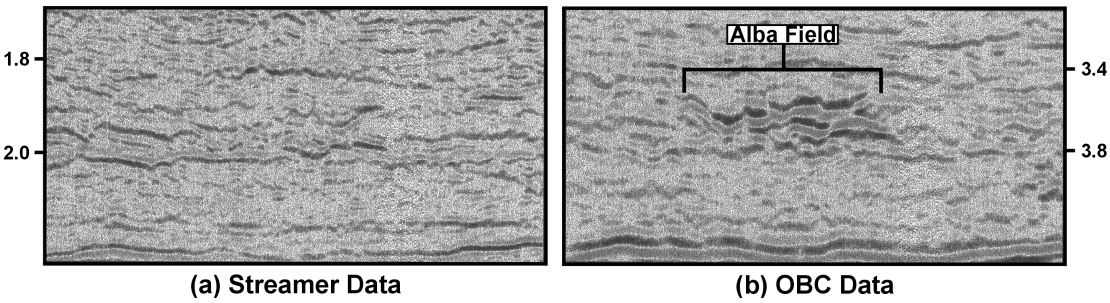

Figure 9. Comparison of (a) streamer data and (b) converted-wave OBC data from the Alba field, North Sea. The converted-wave data provides a much clearer image of the reservoir interval (modified from MacLeod et al., 1999).

showed that this strong S-wave impedance contrast, not surprisingly, gave rise to a strong converted-wave or P-S reflection from the top of the reservoir.

Based on these modelling results, Chevron and its partners were motivated to acquire a 67 km^2 4C-3D survey of the Alba field which produced very striking results. As illustrated in Figure 9, the converted-wave or P-S data showed a greatly improved image of the reservoir as compared with the P-P image in almost every part of the Alba field (MacLeod et al., 1999).

ATTENUATION OF FREE-SURFACE MULTIPLES

A number of interesting methods for attenuating free-surface multiples have been developed recently. Like the dual-sensor idea, these methods can be developed using *z* transform theory.

One of the most general methods is described by Berkhout and Verschuur (1997) and Weglein et al. (1997). Weglein (1997) gives a clear explanation of this method using inverse scattering theory. The method can be understood by examining the free-surface reflections in terms of the upcoming wavefield as in equation (4). Instead of a single reflection *R*, consider *R(Z)* as the *z* transform of the reflectivity sequence:

$$U(Z) = \frac{R(Z)}{1 + R(Z)} \tag{13}$$

In this equation, *U(Z)* is equivalent to $R_f(Z)$ in Weglein (1999).

We can rewrite (13) in terms of a series in *U(Z)*:

$$\begin{aligned} U(Z)\left[1 + R(Z)\right] &= R(Z) \\ R(Z)\left[1 - U(Z)\right] &= U(Z) \\ R(Z) &= \frac{U(Z)}{1 - U(Z)} \end{aligned} \tag{14}$$

Expanding the series given by equation (14), we arrive at:

$$\begin{aligned} R(Z) &= U(Z)\left[1 + U(Z) + U^2(Z) + \ldots\right] \\ &= U(Z) + U^2(Z) + U^3(Z) + \ldots \end{aligned} \tag{15}$$

It is interesting to note that the upcoming reflectivity series of primaries and internal multiples, *R(Z)*, can be expressed in terms of infinite series of the total upgoing wavefield in the presence of a free-surface, *U(Z)*.

Equation (15) states that the reflectivity sequence, *R(Z)*, can be constructed by successive convolutions of the total wavefield with itself (i.e. *U(Z)*, $U^2(Z)$, $U^3(Z)$, …). This extraction of reflectivity from the total wavefield can be achieved by surface recording (and without any subsurface model assumptions) with Weglein's inverse scattering approach. However, it does assume a stationary behaviour to the multiple sequence.

A multiple suppression scheme which utilises both surface and OBC recording is given by Ikelle (1999). The derivation of Ikelle's method can be obtained by recalling Weglein's analysis. In Weglein's inverse scattering analysis given by equation (14), we *see* that the total reflectivity can be generated by adding higher order terms in the recordings of free-surface multiples.

Ikelle (1999) shows that a similar inverse scattering relationship holds for the OBC recording. If *D(Z)* is the OBC wavefield and *U(Z)* is the upgoing wavefield recorded at the surface, then $D(Z) = Z^{1/2}U(Z)$. That is, the OBC recording is a time-delayed version of the surface recording. Also, the upgoing compressions change to downgoing rarefractions at the free-surface, and vice-versa. For the geophones located in the ocean-bottom sensor $D(Z) = Z^{1/2}U(Z)$ and for the hydrophone $D(Z) = -Z^{1/2}U(Z)$. Therefore, it is not surprising that the inverse scattering relationship given by Ikelle (1999) is similar to Weglein (1999). That is,

$$D_p(Z) = D_0(Z) + D_1(Z) + D_2(Z) + \ldots \tag{16}$$

where $D_p(Z)$ is the reflectivity sequence expressed in terms of higher order multiple sequences. This is equation (1) from Ikelle (1999) without the source wavelet term (we consider the source wavelet deconvolution to be a separate problem). Ikelle (1999) shows that the OBC sequence of higher order multiples (i.e. $D_1(Z)$, $D_2(Z)$, …) can be generated by combining both OBC and streamer data.

A simple example of Ikelle's relationship between the OBC and streamer recording is shown in Figure 10. Consider a water layer with one-way propagation time t_1 overlying a rock layer of one-way propagation time t_2. Using Ikelle's notation consider the following arrivals as in Figure 10, we define:

D_0 = arrivals at OBC which are direct or primary reflection arrivals,

E_0 = arrivals at streamer which are direct or primary reflection arrivals and

D_1 = arrivals at OBC which are first order receiver ghosts and first order multiples.

The arrivals in D_0 are given by a downgoing compression of unit amplitude at time t_1 and an upgoing compression of unit amplitude R_2 at time $t_1 + 2t_2$. The z transform is given by:

$$D_0(z) = z^{t_1} + R_2 z^{t_1+2t_2} \tag{17}$$

where Z used previously is given by $Z = z^{2t_1} = z^{\tau}$. Recall z relates to the sample interval and Z to the two-way time through the water layer.

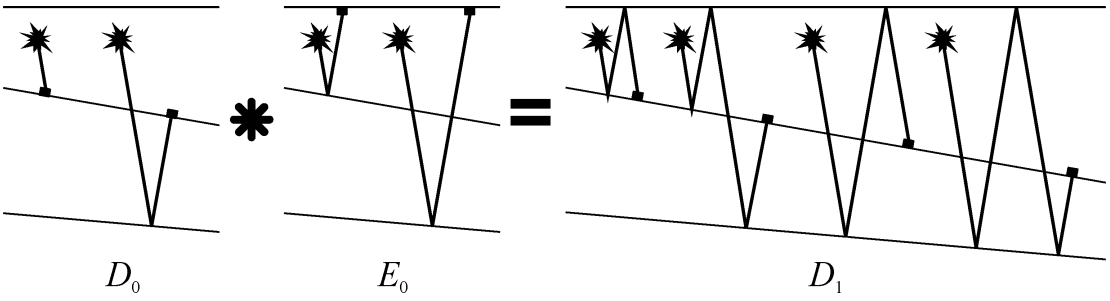

Figure 10. An example of combining streamer and OBC primaries to produce OBC multiples (modified from Ikelle, 1999).

The arrivals in E_0 are given by an upgoing compression of amplitude R_1 at time $2t_1$ and an upgoing compression of amplitude R_2 at time $2t_1 + 2t_2$. The z transform is given by:

$$E_0(z) = R_1 z^{2t_1} + R_2 z^{2t_1+2t_2} \tag{18}$$

The arrivals in D_1 are given by a downgoing rarefraction of amplitude R_1 at time $3t_1$, an upgoing rarefraction of amplitude R_1R_2 at time $3t_1 + 2t_2$, a downgoing rarefraction of amplitude R_2 at time $3t_1 + 2t_2$ and an upgoing rarefraction of amplitude R_2^2 at time $3t_1 + 4t_2$. The z transform is given by:

$$D_1(z) = -R_1 z^{3t_1} - R_1 R_2 z^{3t_1+2t_2} - R_2 z^{3t_1+2t_2} - R_2^2 z^{3t_1+4t_2} \tag{19}$$

Therefore we see that by comparing $D_0(z)E_0(z)$ to $D_1(z)$, we have:

$$\begin{aligned} D_0(z)E_0(z) &= \left(z^{t_1} + R_2 z^{t_1+2t_2}\right)\left(R_1 z^{2t_1} + R_2 z^{2t_1+2t_2}\right) \\ &= R_1 z^{3t_1} + R_1 R_2 z^{3t_1+2t_2} + R_2 z^{3t_1+2t_2} + R_2^2 z^{3t_1+4t_2} \\ &= -D_1(z) \end{aligned} \tag{20}$$

It is interesting to note from equation (20) that higher order multiples measured at the OBC can be generated by using the streamer data and lower order multiples.

The use of the dual fields of displacement and pressure by ocean-bottom geophones and hydrophones to deconvolve multiples is analogous to handling of electric and magnetic fields in electromagnetism. For this reason, the use of dual

fields is called Einstein deconvolution by Loewenthal and Robinson (1999) in their discussion of dual-sensors.

CONCLUSIONS

The use of ocean-bottom seismic recording may prove to be useful for several purposes. We have discussed three of these including dual-sensor summation for suppression of receiver-side multiples, enhanced seismic imaging using converted waves and the attenuation of free-surface multiples through combination of conventional streamer and ocean-bottom cable seismic data. We show that these applications can be understood mathematically through the use of *z* transforms and through applications to synthetic and real data.

ACKNOWLEDGEMENTS

We would like to thank Larry Mewhort of Husky Oil Operations Ltd. and Larry Sydora of Hibernia Management and Development Company Ltd. who generously provided us with well information which aided in the construction of the general elastic wave model of the Jeanne d'Arc Basin. We also thank John Granli and Børge Arntsen of Statoil for providing us with the seismic images of the Tommeliten field. Finally, we thank all sponsors of the CREWES Project for their continued technical and financial support.

REFERENCES

Barr, F. J., and Sanders, J. I., 1989, Attenuation of water-column reverberations using pressure and velocity detectors in a water-bottom cable: 59th Ann. Internat. Mtg., Soc. Expl. Geophys., Expanded Abstracts, 653-656.

Berkhout, A. J. and Verschuur, D. J., 1997, Estimation of multiple scattering by iterative inversion, Part I: Theoretical considerations: Geophysics, **62**, 1586-1595.

Caldwell, J., Kristiansen, P., Beaudoin, G., Tollestrup, K., Siddiqui, S., Wyatt, K., Camp, W. and Raney, G., 1998, Marine 4-component seismic test, Gulf of Mexico: subsalt imaging at Mahogany Field: 67th Ann. Internat. Mtg. Soc. Expl. Geophys. Expanded Abstracts, 2091-9092.

Dragoset, W. and Barr, F. J., 1994, Ocean-bottom cable dual-sensor scaling: 64th Ann. Internat. Mtg., Soc. Expl. Geophys., Expanded Abstracts, 857-860.

Granli, J. R., Arnsten, B., Anders, S. and Hilde, E. 1999, Imaging through gas-filled sediments using marine shear-wave data: Geophysics, **64**, 668-677.

Ikelle, L. T., 1999, Combining two seismic experiments to attenuate free-surface multiples in OBC data: Geophys. Prosp., **47**, 179-193.

Lowenthal, D., Lee, S. S., and Gardner, G. H. F., 1985, Deterministic estimation of a wavelet using impedance type technique: Geophys. Prosp., **33**, 956-969.

Lowenthal, D. and Robinson, E. A., 1999, On unified dual fields and Einstein deconvolution: paper accepted for publication in Geophysics.

MacLeod, M. K., Hanson, R. A., Hadley, M. J., Reynolds, K. J., Lumley, D., McHugo, S., and Probert, A., 1999, The Alba field OBC seismic survey: 61st Ann. Mtg., Eur. Assn. Geosci. Eng., Expanded Abstracts, No. 6-25.

Osen, A., Amundsen, L., and Reiten, A., 1999, Removal of water-layer multiples from multicomponent sea-bottom data, Geophysics, **64**, 838-851.

Paffenholz, J., and Barr, F. J., 1996. An improved method for determining water bottom reflectivities from dual- sensor ocean bottom cable data: 58th Ann. Mtg., Eur. Assn. Expl. Geophys., Expanded Abstracts, 987- 989.

Weglein, A. B. 1999. How can the inverse-scattering method really predict and subtract all multiples from a multidimensional earth with absolutely no subsurface information?: The Leading Edge, **18**, No. 1, 132-136.

Weglein, A. B., Gasparotto, F. A., Carvalho, P. M. and Stolt, R. H., 1997, An inverse scattering series method for attenuating multiples in seismic reflection data: Geophysics, **62**, 1975-1989.

White, J. E., 1975, Computed seismic speeds and attenuation in rocks with partial gas saturation: Geophysics, **40**, 224-232.